JOURNAL OF MATERIALS SCIENCE 16 (1981) 3263–3274

Some measurements of internal stress and activation volume in acrylic polymers

B. HAWORTH*, J. R. WHITE
Department of Metallurgy and Engineering Materials, University of Newcastle-Upon-Tyne, Newcastle-Upon-Tyne, UK

Stress relaxation tests conducted on poly(methyl methacrylate) (PMMA) in various forms have been analysed using the procedure of Kubát and Rigdahl. The values of σ_i, the internal stress parameter, obtained from this analysis are subject to large errors and do not provide useful comparators, nor do they correlate with residual stress measurements made by the layer removal method. The index, n, changes with test temperature in a systematic manner and reveals marked differences in relaxation behaviour between the different classes and specimens investigated. A new method for estimating activation volume from the stress relaxation procedure has been tested and found to give values that are much higher for injection-moulded bars than for "Perspex" sheets as-received or hot-drawn.

1. Introduction

The properties of fabricated polymers are very dependent upon solidification conditions, particularly on orientational flow just prior to solidification and on temperature gradients during solidification. Residual stresses are usually produced as a consequence of non-uniform cooling rates. Molecular orientation is retained if the cooling rate is sufficiently large to prevent randomization of molecular conformation following orientational flow. Injection mouldings show both of these effects and normally possess tensile stresses in the interior and compressive stresses near to the surface [1–13] and at the same time retain significant molecular orientation. We have discussed methods of assessing residual stresses previously [10–13], but have presented little on the effect of orientation [13].

The presence and to some degree the distribution of molecular orientation can be shown by shrinkage tests [1–4, 7, 13]. Bi-refringence is sensitive to both residual stress and orientation although it is the latter that normally dominates. Separation of the two effects has been demonstrated by Saffell and Windle [14] but there still remains difficulties with the use of bi-refringence for characterization. Firstly, the separation procedure used by Saffell and Windle is fairly delicate and time consuming, and hardly lends itself to routine analysis. Secondly, it seems that the major contribution to a change in bi-refringence may sometimes be the consequence of side group re-organization that takes place without conformational changes in the main chain [13, 15–17].

In our own laboratory, we have sought correlations between residual stresses and mechanical properties, using the layer removal procedure to assess residual stresses [10–13]. We have previously reported some preliminary work on the assessment of orientation in polystyrene mouldings by bi-refringence measurements [13]. As part of our initial studies, we performed stress relaxation tests and derived the "internal stress parameter" according to the procedure of Kubát and Rigdahl ("KR") [18]. This quantity is supposed to be representative of the residual stress level within the specimen [18–20] but is sensitive to differences in structure and relaxation behaviour from one position to another [19]. Part of the purpose of the work described here was to see whether it is possible to reconcile the KR internal stress parameter with measured residual stress levels using independent measurements of stress relaxation behaviour of isotropic and oriented material. We also intended to test predictions of an alternative theory based on the site model approach to stress-aided thermally activated deformation behaviour [21, 22].

0022–2461/81/123263–12$03.20/0

2. Experimental procedure

2.1. Specimen preparation

2.1.1. Injection moulding

Specimens were injection-moulded from ICI Diakon MG 102 acrylic polymer with a Butler-Smith 100/60 reciprocating screw machine using an injection pressure of 129 MPa, Zone 1/Zone 2/ nozzle temperatures of 195/240/225° C, a mould temperature of 20° C and a cooling time of 25 sec. Several specimens were rejected after the machine had settled down to cycling at a constant rate under nominally fixed conditions before collecting specimens for testing. Each specimen was given a serial number in order that any change in property associated with drift in moulding conditions could be detected subsequently. The tool cavity was end-gated and produced bars measuring approximately 190 mm × 12.7 mm × 3.1 mm.

2.1.2. Drawn specimens

The work reported here was conducted on specimens provided by ICI Plastics Division and were prepared as follows: test bars were cut from a 3 mm thick "Perspex" sheet and drawn in a hot chamber at 130° C on an Instron tensile testing machine using a cross-head speed of 50 mm min^{-1} and an initial grip separation of 50 mm. The cross-head was arrested at a draw ratio of 3 : 1 and the specimen cooled rapidly to 50° C using an air blower while still under tension. The specimen was then allowed to cool slowly to ambient temperature.

2.1.3. Isotropic specimens

Specimens representative of isotropic material were machined from a 19 mm thick "Perspex" sheet. The machined surfaces were polished on a polishing wheel using alumina powder carried on a synthetic cloth. Lubrication and cooling of the surface was provided during polishing by a plentiful supply of water and "Teepol" detergent. Specimens were examined between crossed polars in all directions and were found to be sufficiently free from bi-refringence to justify the use of the description "isotropic".

2.2. Layer removal procedure

The residual stress distribution was determined by the layer removal procedure [10–13, 23, 24]. Uniform layers were removed from the bar by high-speed milling. The curvature that resulted from the consequent imbalance of forces through the bar was measured using the laser technique described previously [11]. The analysis of the curvature against depth removed data, to produce residual stress profiles, again made use of the assumption that the modulus was uniform throughout the bar.

2.3. Stress relaxation

Stress relaxation experiments were conducted in both tension and compression on rigs designed and built for this purpose [11, 25]. The load cells (Pye Ether UF2) used on the rigs are bi-directional so that the only modification required to accommodate compression testing was to replace the wedge grips with cylindrical anvils with flat ends [25].

For a tensile experiment, the specimen was mounted on the bench prior to testing and the grips tightened without applying a load to the specimen [11]. Injection-moulded bars were used as-moulded. Specimens cut from isotropic sheets of material measured 88 mm × 8 mm × 4 mm and those cut from drawn samples measured 50 mm × 4 mm × 3.5 mm. For compression tests, specimens were normally cut to a length of 6 to 7 mm to prevent buckling under load.

The thermal cabinet was re-designed to accommodate short specimens as used in compression for which the sensitivity to temperature fluctuations is much greater [25]. The specimen was allowed to temperature-equilibrate in the thermal cabinet for 30 min prior to the application of the deformation.

2.4. Bi-refringence measurements

Injection-moulded specimens were of high optical transparency and were used as-moulded. For other specimens, cut surfaces had to be prepared by polishing as described earlier. Values of relative retardation were estimated by identifying the characteristic colour corresponding to the optical path difference caused by the double refraction of polychromatic light in the specimen. For this purpose, a polarizing microscope was used in conjunction with a quartz wedge compensator.

All specimens were inspected between crossed polars prior to mechanical testing and it was confirmed that the injection mouldings were identical at least in their bi-refringence. Specimens made out of the drawn material were cut from a region of uniform bi-refringence.

2.5. Annealing and shrinkage tests

Selected specimens were placed in an air oven at elevated temperatures for varying periods. The

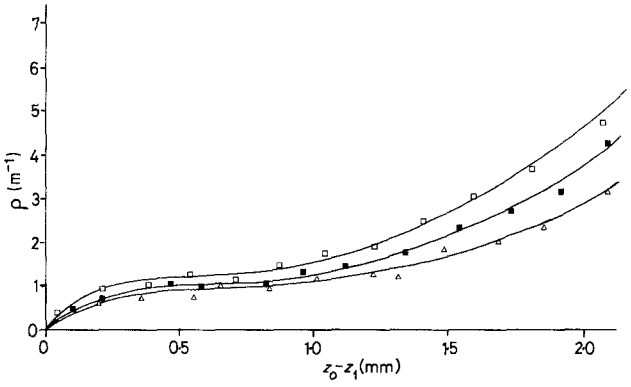

Figure 1 Curvature (ρ) against depth removed ($z_0 - z_1$) for (i) as-moulded bar (□), (ii) bar annealed for 5 h at 71° C (■) and (iii) bar annealed for 5 h at 96° C (△).

purpose of these experiments was firstly to see if any marked changes occurred during thermal treatments similar to those experienced in a stress relaxation test; secondly, to see if the residual stress level could be altered without producing significant shrinkage; and thirdly, to examine the shrinkage characteristics of the mouldings.

3. Results

3.1. Layer, removal experiments

3.1.1. Effect of annealing

Figs 1 and 2 show the results obtained with an as-moulded bar and with bars annealed at 71 and at 96° C, respectively. Curvature against depth removed is plotted in Fig. 1 and the corresponding residual stress profiles computed from these curves are shown in Fig. 2. The stress is tensile in the interior and compressive near to the surface, rising at quite large values at the surface (about 30 MN m^{-2} for the as-moulded sample). Annealing is seen to reduce the curvature produced for any thickness removed and the analysis confirms that the overall residual stress level diminishes.

3.1.2. Drawn samples

Because of a shortage of specimens only one layer-removal test was conducted with a drawn sample. The as-prepared specimen already had a significant curvature and was therefore not typical so a full analysis using small layer-removal increments was not attempted. From the results of two large increments it was indicated that substantial stresses were present: about 13 to 14 MN m^{-2} (compressive) at the surface and 6 to 7 MN m^{-2} (tensile) in the centre. It is likely that all drawn specimens contained stresses of this order but the exact magnitudes would depend on the cooling rate, which was not controlled. Uneven cooling was probably the cause of the initial curvature in the as-prepared bar.

3.2. Stress relaxation

3.2.1. Effect of temperature

Stress relaxation tests conducted at 50, 70 and 80° C all showed the familiar sigmoidal stress (σ) against ln time (t) characteristic (Fig. 3), with the position of the point of inflection moving to smaller times with increasing temperature. This is of course as predicted by most theories, including the site model theory [21, 22].

3.2.2. Compression testing

Specimens tested in compression showed a much larger time constant than those tested in tension (Fig. 4).

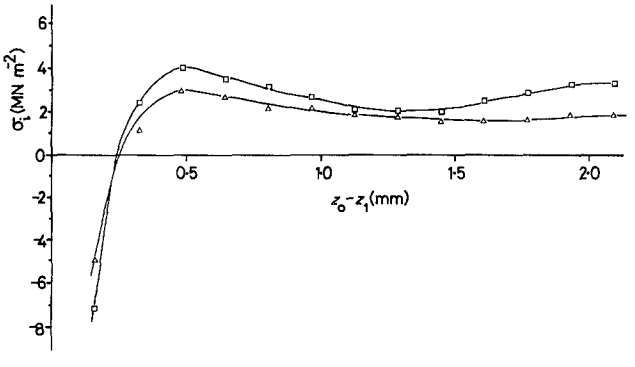

Figure 2 Computed residual stress distributions (σ_i) for (i) as-moulded bar (□) and (iii) bar annealed at 96° C (△).

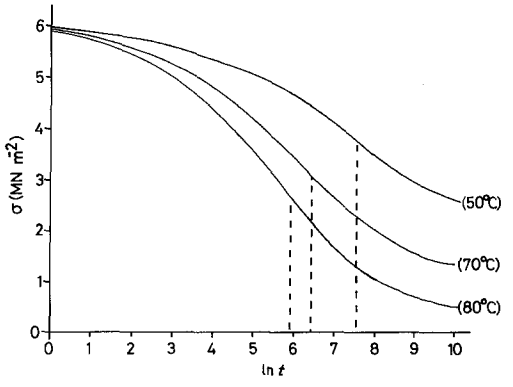

Figure 3 Stress relaxation in tension for similar σ_0 values at three different temperatures. (Injection-moulded "Diakon".)

3.2.3. KR plots

Samples from each batch of nominally identical specimens were tested at different deformations and the steepest gradient for each σ against $\ln t$ plot was recorded. This gradient was plotted against the initial stress for each specimen in a particular batch, according to the procedure of Kubát and Rigdahl (KR) [18]. The results are shown in Figs 5 to 8; in these figures the following points are illustrated:

(i) the effect of temperature (Fig. 5: the specimens are injection mouldings);

(ii) the effect of compression compared with tension testing (Figs 6, 7 and 8);

(iii) differences between different classes of materials (compare Figs 6, 7 and 8).

The scatter in some of the data is considerable and

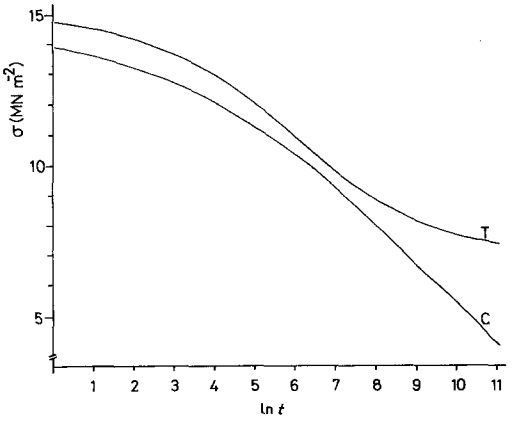

Figure 4 Stress relaxation in tension (T) and compression (C) for similar initial stress magnitudes. Both tensile and compressive stresses are plotted as positive. The point of inflection occurs after approximately 5 min ($\ln t \sim 6$) in tension, but after a much longer time in compression.

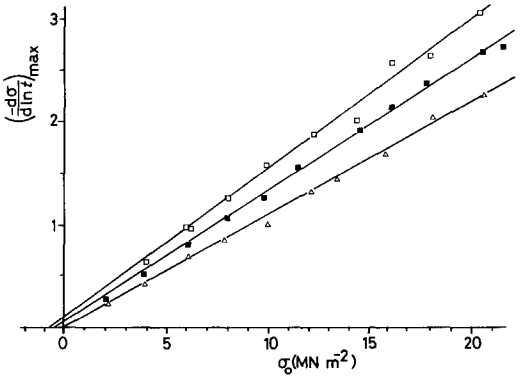

Figure 5 KR plots for injection-moulded PMMA bars tested in tension at 50° C (△), 70° C (■) and 80° C (□).

this is reflected in the standard deviations estimated from a regression analysis used to locate the best straight line from the data points, see Table I. The results are presented in terms of the intercept on the σ_0 axis (called by Kubát and Rigdahl the "internal stress parameter", σ_i) and the power-law index, n. Although n strictly has a significance only as long as the power law is valid its value as estimated from the gradient of the KR plots ($= n^{-n/(n-1)}$), has been found to be a promising characteristic for injection mouldings [10, 13].

3.2.4. Activation volume analysis

In a previous paper [22] arguments were presented for rejecting the identification of the quantity $[\mathrm{d} \ln (-\dot{\sigma})/\mathrm{d}\sigma]$ with the activation volume. Instead a new analysis was introduced in which the use of the site model theory led to the prediction that a plot of $1/\sigma_i$ against $1/(\sigma_0 - \sigma_i)$ should give a straight line with gradient M and intercept c on the $1/\sigma_i$ axis where σ_0 is the initial stress in the stress relaxation test and σ_i is the final equilibrium

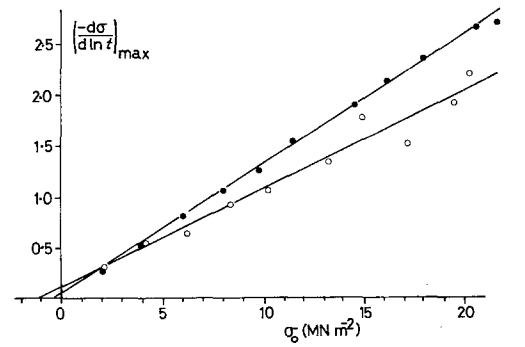

Figure 6 KR plots for injection-moulded PMMA bars tested at 70° C in tension (•) and compression (○). Both tensile and compressive stresses are plotted as positive.

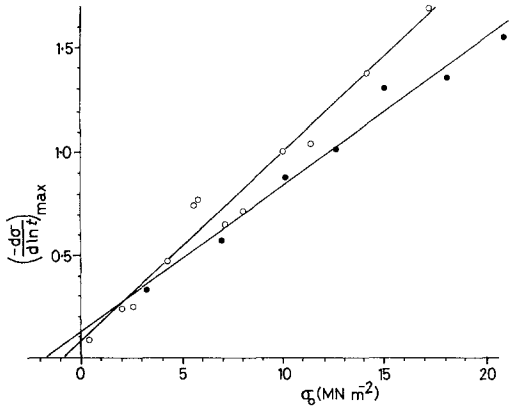

Figure 7 KR plots for drawn "Perspex" tested at 70° C in tension (•) and compression (○). Both tensile and compressive stresses are plotted as positive.

stress (= deformation-induced internal stress). Reference to the previous paper [22] shows that M and c are given by the following expressions:

$$M = \left(\frac{V_{12} + V_{21}}{kT}\right) \frac{N_1^0 \, \Delta\sigma}{(1 + \exp \delta\Delta G/kT)} \quad (1)$$

and

$$c = \left(\frac{V_{12} + V_{21}}{kT}\right) \frac{\exp \delta\Delta G/kT}{(1 + \exp \delta\Delta G/kT)} \quad (2)$$

so that

$$\frac{M}{c} = \frac{N_1^0 \, \Delta\sigma}{\exp \delta\Delta G/kT}, \quad (3)$$

where $\delta\Delta G$ represents the difference in energy between the two sites for the jumping element, N_1^0 is the population of type "Site 1" in the unstressed state, $\Delta\sigma$ is the incremental stress decay per unit change in site population, V_{ij} is the activation volume for a jump in the direction $i \rightarrow j$, ($V_{ij}\sigma$ is the change in barrier height produced by an applied stress, σ), k is the Boltzmann constant and T is the absolute temperature.

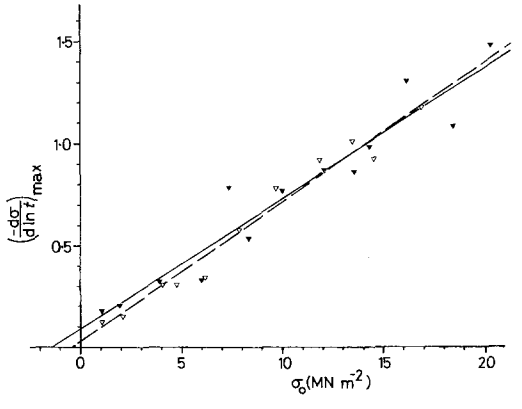

Figure 8 KR plots for as-received "Perspex" tested at 70° C in tension (▾) and compression (▽). Both tensile and compressive stresses are plotted as positive.

The site model theory also predicts that $\sigma_i \propto \sigma_0$ so that a plot of σ_i against σ_0 should be a straight line passing through the origin with slope $1/(1 + M)$.

In order to exploit this analysis values for σ_i must be obtained for each stress relaxation experiment. To obtain this value directly would take an unacceptably long time (> 24 h for each specimen tested, even in the tensile experiments) and we have instead used two simple extrapolation methods. Firstly we have employed the method introduced by Li [26] and also used for polymers by Kubát and co-workers [20, 27, 28]. Here a plot of $(-\mathrm{d}\sigma/\mathrm{dln}\, t)$ against σ is constructed and σ_i is taken to be the intercept on the σ axis, for at this point $(\mathrm{d}\sigma/\mathrm{dln}\, t)$ is zero and the limiting stress has been reached. The power law predicts that this plot should be a straight line, making extrapolation convenient. On the other hand, we have reservations about the power law and have therefore explored the possibility of providing a routine for estimating σ_i based on the results of the site model analysis [22] and this has given the second technique as follows:

The site model theory leads to the $\sigma(t)$ relationship [22]

$$\sigma = \sigma_0 \exp(-Ct) + \frac{D\sigma_0}{C}[1 - \exp(-Ct)], \quad (4)$$

where C and D are functions of the temperature and activation parameters. It follows that

$$\frac{\mathrm{d}\sigma}{\mathrm{dln}\, t} = -Ct\left(\sigma - \frac{D\sigma_0}{C}\right) = -Ct\,(\sigma - \sigma_i). \quad (5)$$

Hence, a plot of $[(-1/t)(\mathrm{d}\sigma/\mathrm{d}\ln t)]$ against σ should be a straight line with intercept $\sigma = \sigma_i$ on the σ axis. This is of course in contradiction to the Li [26] analysis; In the event both plots turn out to be curved, (in opposite senses) (Figs 9 to 11). The Li [26] analysis can only apply to the long-term part of the σ against ln t curve after the point of inflection. If results at shorter times are included the Li plot goes through a maximum, as can be seen in the examples given in Figs 9 and 10. For long times the plot comes down quite steeply, giving a reasonably precise interception with the σ axis. The $[(-1/t)(\mathrm{d}\sigma/\mathrm{d}\ln t)]$ against σ plot falls a little less steeply, but also gives a fairly

TABLE I

Material	State	Average birefringence ($\times 10^4$)	Test temperature (° C)	T or C*	σ_i(KR [18]) (MN m^{-2})	σ_i(Li [26]) (MN m^{-2})	n	ckT ($\times 10^{30}$ m^3)
Perspex	As-received	−0.35	70	T	−1.31 ± 1.32	0.1 ± 0.2	12.0 ± 1.5	150 ± 100
	("isotropic")	−0.35	70	C	0.28 ± 0.64		11.2 ± 0.9	
Perspex	Hot-drawn	−8.44	70	T	−1.80 ± 1.12	1.3 ± 0.7	10.8 ± 0.9	270 ± 80
		−9.79	70	C	0.80 ± 0.64		8.1 ± 0.7	
Diakon	Injection-moulded	−0.56	70	T	−0.40 ± 0.26	0.3 ± 0.2	5.4 ± 0.1	430 ± 70
		−0.56	70	C	1.14 ± 1.24		7.7 ± 0.8	
		−0.56	50	T	0.04 ± 0.28	0.8 ± 0.2	6.6 ± 0.2	530 ± 310
		−0.56	80	T	−0.73 ± 0.69	0.02 ± 0.03	4.6 ± 0.3	1000 ± 670

*T = tension, C = compression.

precise interception with the σ axis in Figs 9 and 10. The intercepts of both plots are in good agreement for a particular relaxation curve and values of σ_i have been chosen using both plots for guidance. Much more pronounced curvature is found in the plots obtained for injection mouldings (Fig. 11) and values of σ_i are not easily estimated. This may be the consequence of having a specimen containing regions of quite different structure, with different states of orientation and probably different amounts of free volume, each with a different relaxation behaviour.

Reasonably straight lines have been obtained for the $1/\sigma_i$ against $1/(\sigma_0 - \sigma_i)$ and the σ_i against σ_0 plots (Figs 12 and 13). This is, of course, a condition of linear viscoelastic behaviour, with which our data displays only partial agreement.

To obtain an estimate of the activation volume it is convenient to start with the expression for c, (Equation 2). We observe that if $\delta\Delta G$ is positive then

$$2ckT \leqslant (V_{12} + V_{21}) \leqslant ckT. \qquad (6)$$

From the plots of $1/\sigma_i$ against $1/(\sigma_0 - \sigma_i)$ we obtain values of ckT shown in Table I.

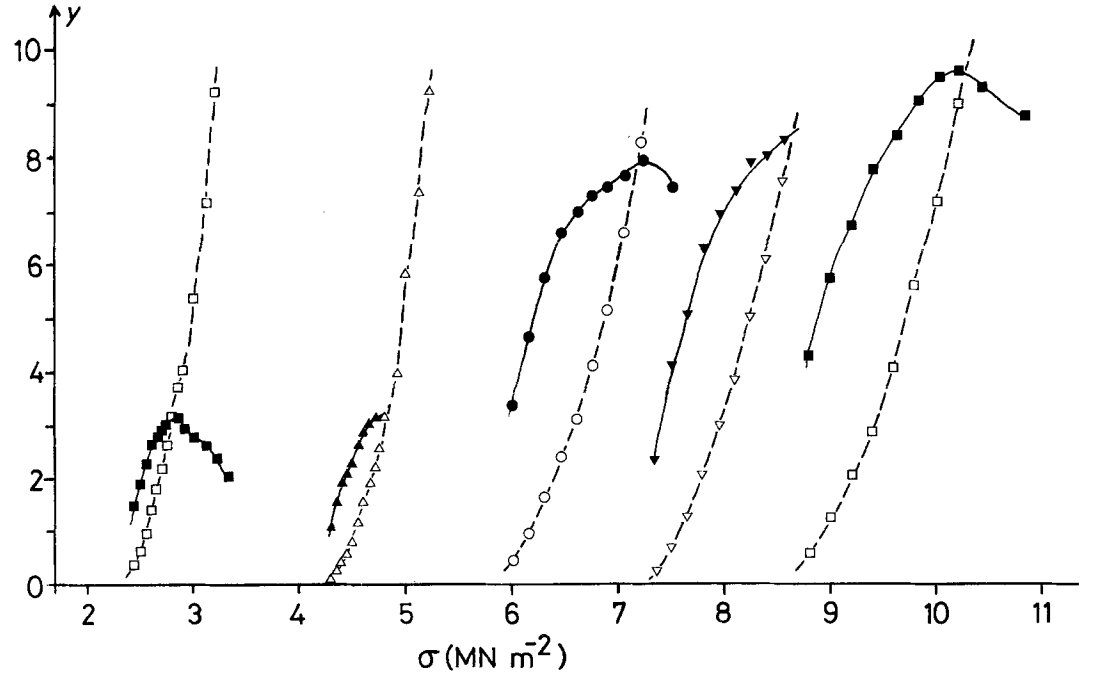

Figure 9 Example of Li [26] plots (solid symbols; $y = -10\ \mathrm{d}\sigma/\mathrm{d}\ln t$) and of the corresponding $y = [(-1/t)(\mathrm{d}\sigma/\mathrm{d}\ln t)]$ against σ plots [open symbols; $y = (-10^4/t)/(\mathrm{d}\sigma/\mathrm{d}\ln t)$] where σ is in MN m^{-1} and t is in sec. "Diakon" injection mouldings tested at 70° C.

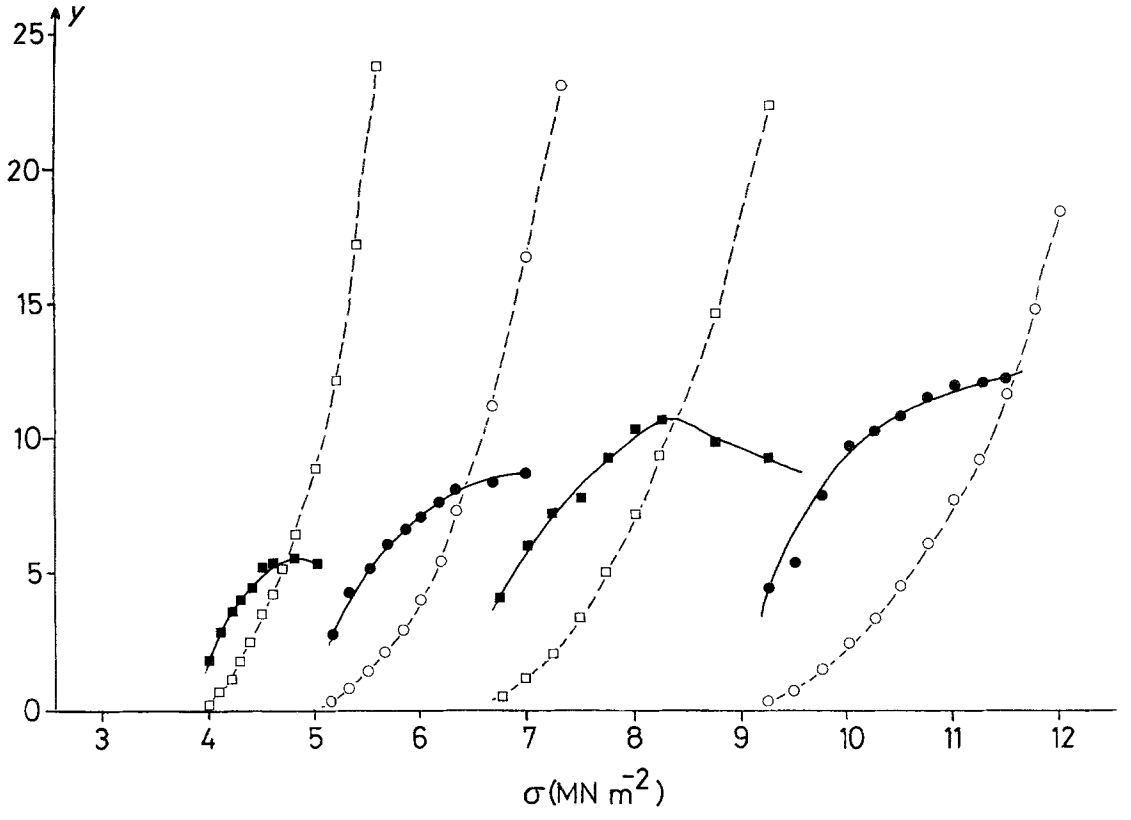

Figure 10 As Fig. 9, but for drawn "Perspex" samples tested at 70° C.

The logical conclusion of this analysis is to rearrange Equation 3 to give

$$\frac{\delta\Delta G}{kT} = \ln\frac{c}{M} + \ln N_1^0\,\Delta\sigma. \qquad (7)$$

Hence, a plot of $\ln c/M$ against $1/T$ should give $\delta\Delta G/k$ as gradient and confirm the sign of $\delta\Delta G$ as well as indicating its magnitude. The fractional errors in the intercepts, c, are large since the intercepts in the $1/\sigma_i$ against $1/(\sigma_0 - \sigma_i)$ plots are quite close to the origin, also, the use of Equation 7 is further limited because only a fairly narrow range of temperature can be investigated conveniently. Nevertheless an attempt to perform such an analysis has been made with the data from injection-moulded PMMA and is illustrated in Fig. 14. The difficulty in drawing conclusions from such a plot is apparent, but it does seem that the gradient is positive, as required if $\delta\Delta G$ is positive and so justifies the use of the limit expression Equation 6.

3.4. Bi-refringence and shrinkage

The change in bi-refringence produced by annealing a drawn sample for 2 h at different temperatures is shown in Fig. 15, along with longitudinal shrinkage measurements.

4. Discussion

4.1. Stress distribution and the effect of annealing

The layer-removal experiments showed that the injection moulded "Diakon" polymer contained moderate tensile residual stresses in the interior ($\sim 4\,\mathrm{MN\,m^{-2}}$ in the as-moulded state), and substantial compressive residual stresses near to the surface (rising to about $30\,\mathrm{MN\,m^{-2}}$ in the as-moulded state). The stress magnitude falls off rapidly on moving in from the surface of the 3 mm thick bar and reverses sign within 0.3 mm. The tensile stress rises rapidly to a maximum, falls slightly, then stays fairly steady through the core region. This is in contrast to many examples of as-moulded polystyrene bars in which the stress distribution has been found to be fairly close to the classic parabolic shape predicted by approximate calculations [12, 13, 25]. On the other hand, the use of different moulding conditions with polystyrene seems to alter the distribution of stress more than the

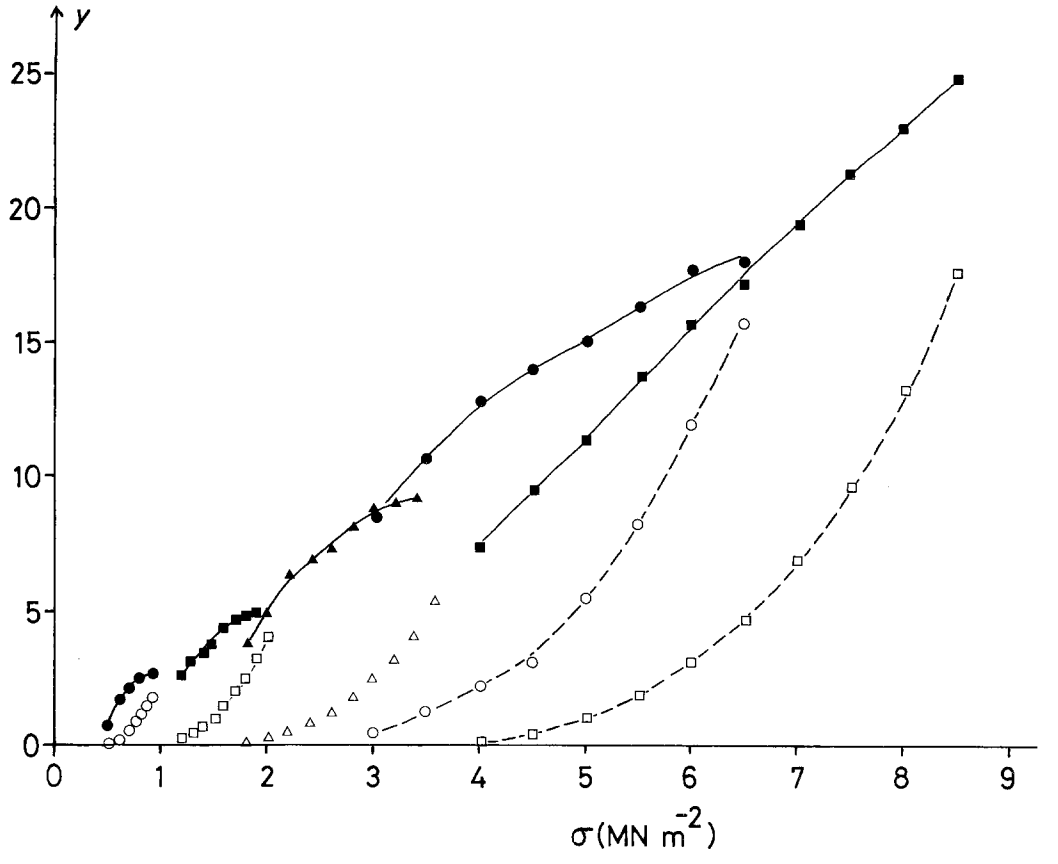

Figure 11 As Fig. 9, but for "Diakon" injection mouldings tested at 70° C. For the open symbols $y = [(-5 \times 10^3/t)] \times (d\sigma/d \ln t)$.

overall magnitudes and until we explore more moulding conditions with PMMA it is not possible to designate the differences in stress distribution as material-specific.

Annealing PMMA has been shown to lower the stress magnitude at all locations but the shape of the distribution remains more or less unchanged, with a broad tensile plateau in the interior, flanked by a steep stress gradient on either side, with strong compressive stresses near the surface. It is interesting to note that the effect of annealing polystyrene injection moulded bars is to produce a similar profile, even to the extent of developing a modest maximum between the point of stress reversal and the tensile plateau, this result having been observed with bars for which the as-moulded stress distribution was fairly close to parabolic [13, 25].

The annealing conditions used for experiments investigating the extent to which residual stresses could be removed without markedly altering the dimensions of the injection mouldings were chosen with reference to the shrinkage data (Fig. 15), and were confined to the region in which shrinkage is negligible. The onset of shrinkage coincides with main chain conformational changes in regions containing oriented molecules and it is notable that significant reduction in the magnitude of the bi-refringence takes place before this is detected (Fig. 15). The same has been observed with polystyrene [13, 25], and it seems that side group re-orientation causes the changes in bi-refringence. In the case of PMMA the process giving rise to the β relaxation should occur readily at the test temperatures employed here and is thought to be associated with motion of the highly polarizable ester side group [29].

4.2. Stress relaxation: KR analyses

In order to explain the stress relaxation behaviour of an injection-moulded bar, it is necessary to know the stress relaxation behaviour of its several morphological constituents. In the case of a glassy polymer it may be sufficient to consider a simple skin-core combination with only two distinct material forms. Kubát and Rigdahl have used a

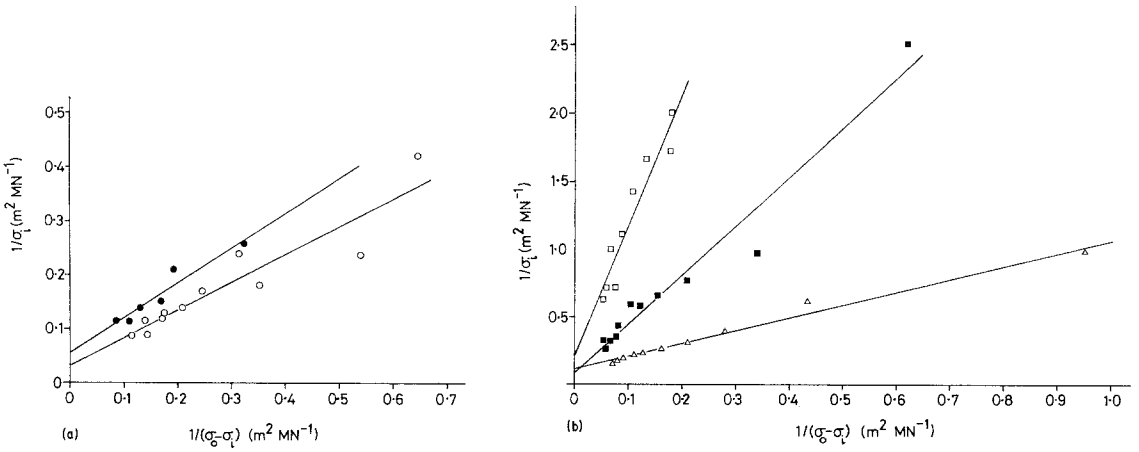

Figure 12 Plots of $1/\sigma_i$ against $1/(\sigma_0 - \sigma_i)$; (a) as-received "Perspex" (○) and drawn "Perspex" (●) tested in tension at 70° C and (b) injection-moulded "Diakon" tested in tension at 50° C (△), 70° C (■) and 80° C (□).

three-layer model, characterizing each layer by a different power-law index "n", and computed the form of KR plots for several combinations of n values and selected residual stress profiles [19]. One of our objectives was to perform a similar analysis and the reason for studying drawn and isotropic "Perspex" was to provide information representative of the (oriented) skin and the (slowly cooled) core, respectively. In the event, the values for n obtained with drawn and undrawn "Perspex" are reasonably close and are well separated from that obtained with the "Diakon" injection mouldings. It is therefore not possible to use our "Perspex" data in the type of analysis employed by Kubát and Rigdahl [19] and obtain agreement with the "Diakon" results. In surveying these results it must be admitted that the "Diakon" injection-moulding grade contains processing aids that are not specified by the manufacturer. The additives in "Perspex" are likely to be quite different and it may be that the parameters investigated in the present study are sensitive to the kind and concentration of these additives.

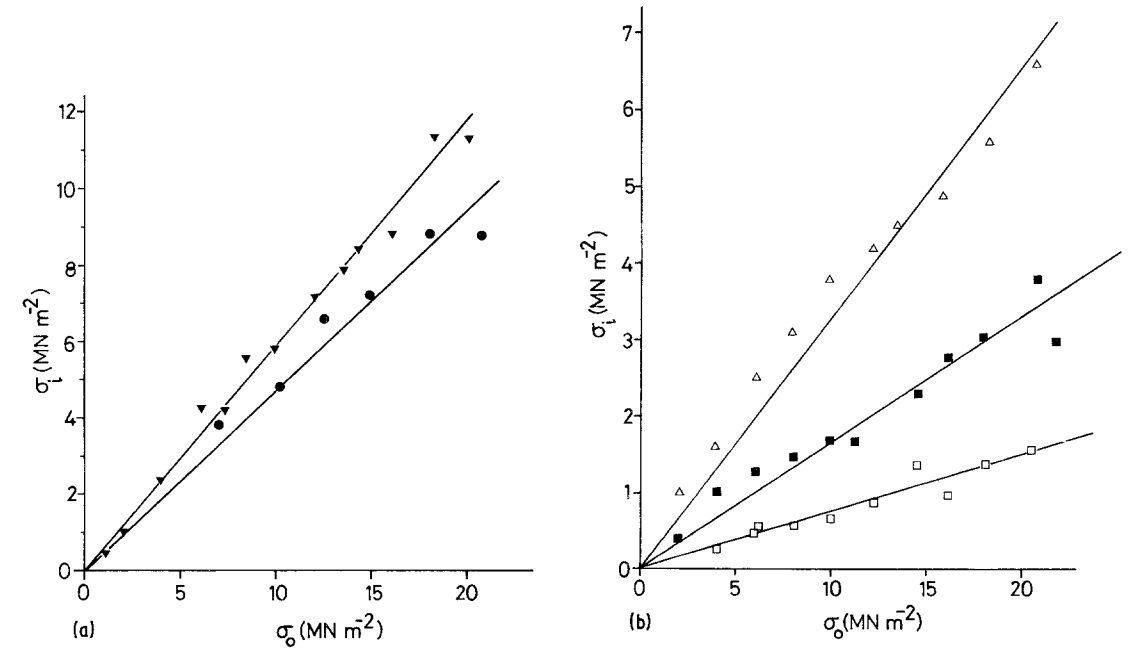

Figure 13 σ_i against σ_0 plots; (a) as-received "Perspex" (▼) and drawn "Perspex" (●) tested in tension at 70° C and (b) injection-moulded "Diakon" tested in tension at 50° C (△), 70° C (■) and 80° C (□).

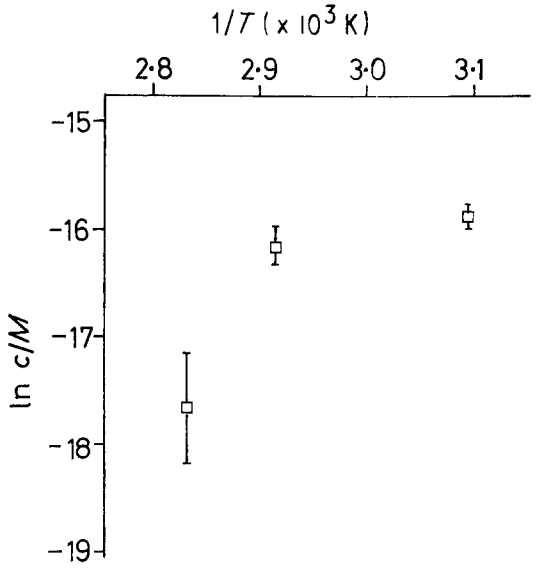

Figure 14 Plot of ln c/M against $1/T$. M is dimensionless and c is in $(\mathrm{MN\ m^{-2}})^{-1}$.

Fig. 3, showing the effect of temperature on stress relaxation, illustrates why 70° C was chosen for the majority of our tests. Lower temperatures would require extremely long times and we have chosen this compromise (as have others before [18]), even though the residual stresses decay at this temperature, as shown by the layer-removal experiments. This does not matter when dealing with the site model theory, but it is not clear how the power law should be affected. The KR plots shown in Fig. 5 show quite clearly that this analysis is sensitive to temperature and that the choice

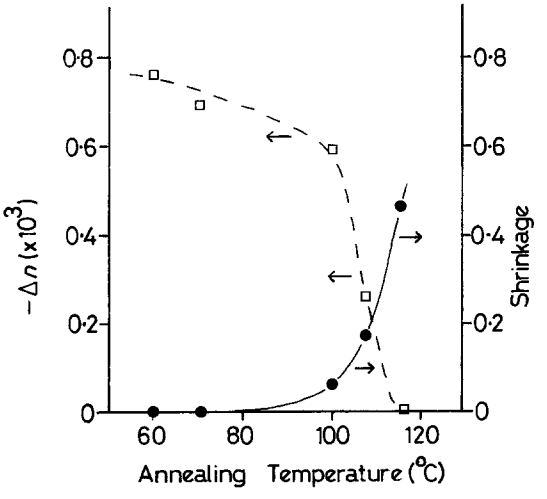

Figure 15 Average bi-refringence (Δn) and longitudinal shrinkage as a function of temperature for drawn "Perspex".

of test temperature is more important than was suggested in the paper describing the method [18].

The analysis of compressive stress relaxation has been conducted in a manner exactly as for tensile stress relaxation and, for convenience, compressive stress has been plotted as positive for all tests. The KR plots derived from the compressive data show similar trends to those obtained in tension and this analysis would appear to be equally valid in tension or compression. Because of the sign convention used the sign of the intercept on the σ_0 axis has been reversed before presenting as σ_i in Table I. Pairs of values of σ_i obtained from compression and tension testing respectively should therefore be equal if σ_i is a truly meaningful parameter. The standard deviation bands overlap but that is about as far as the agreement goes. The values of the parameter n show the same trend in tension and in compression with that for the as-received "Perspex" being the largest and that for "Diakon" the smallest for both loading conditions. The value of n decreases monotonically with test temperatures for the injection mouldings.

4.3. Further analysis of the Li [26] plots

The values for σ_i obtained using the Li [26] analysis are plotted against σ_0 in Fig. 13. In constructing the best straight line through the origin it has been assumed that σ_i contains no component from residual stress. If, on the other hand, σ_i contains a residual stress component that is constant for a particular batch of specimens, this value can be obtained by extrapolating the σ_i against σ_0 plot to intersect with the σ_i axis [10]. By re-computing the data presented in Fig. 13, removing the restriction that the lines should pass through the origin, intercepts have been obtained and are shown in Table I. There is clearly no correlation between the σ_i values obtained in this way and those obtained in the Kubát and Rigdahl analysis. The material used when this analysis was attempted previously [10] was semi-crystalline, with T_g, the glass transition temperature, below room temperature (= test temperature). This may be the reason why a greater degree of agreement was found with this procedure in the previous study.

Since the Li [26] analysis and the Kubát and Rigdahl [18, 19] procedure are both based on the same power law, and, effectively, on the same assumptions regarding the behaviour of σ_i, it is to be expected that better agreement should follow.

4.4. Activation volume

If it is assumed that $\delta\Delta G$ is positive for the isotropic and drawn PMMA samples as well as for the injection mouldings, then the values of the activation volume estimated by our new procedure are quite different for "Perspex" (both in isotropic and oriented form) and for "Diakon".

Inspection of our results leads us to conclude that $\delta\Delta G$ for "Diakon" is sufficiently high to make valid the approximation $(V_{12} + V_{21})/2 = \bar{V} = ckT/2$ so that the activation volumes are not as large as those found in the literature [30, 31]. The spread of values is much smaller than that recorded in the literature [20, 30–42] and we regard this as an indication of the superiority of our analysis. Furthermore our values are roughly consistent with the simple interpretation that activation volume can be equated to the volume swept out by the moving element during a conformational change. This part of the analysis is, of course, incompatible with the power law upon which the KR analysis used in the other sections is based.

5. Conclusions

(a) Residual stresses can be relieved at least partially in PMMA by annealing at temperatures below T_g and this can be achieved without the promotion of shrinkage in specimens containing molecular orientation.

(b) Bi-refringence changes more rapidly than shrinkage on annealing at temperatures below T_g.

(c) Stress relaxation analyses based on the Kubát and Rigdahl procedure and the site model theory are sensitive to the grade of polymer (probably because of additives) and/or to fabrication conditions. For this reason, we were unable to fulfill our initial objective of using stress relaxation data from oriented/isotropic PMMA to predict the behaviour of a skin/core injection-moulded sample.

(d) We have been unable to reconcile results obtained by KR analyses on data obtained in tension and compression, respectively.

(e) σ_i values derived by the KR procedure are subject to large errors in this investigation and also disagree with those obtained by Li analyses (appropriately extrapolated to $\sigma_0 = 0$). The index n does appear to vary in a systematic fashion, however, decreasing as the test temperature increases. Results obtained with polystyrene have also indicated that n may be a useful characteristic but that σ_i is not [12, 13].

(f) We have tested a new method for estimating activation volume, based on the site model theory and have obtained reasonable results.

References

1. W. KNAPPE, *Kunststoffe* **51** (1961) 562.
2. A. PEITER, *Plastverarbeiter* **16** (1965) 664.
3. *Idem, ibid.* **16** (1965) 728.
4. *Idem, ibid.* **17** (1966) 24.
5. *Idem, ibid.* **18** (1967) 883.
6. *Idem, Gummi. Asbest. Kunststoffe* **19** (1966) 1450.
7. S. WINTERGERST, *Kunststoffe* **63** (1973) 636.
8. D. BÜRKLE, *ibid.* **65** (1975) 25.
9. M. RIGDAHL, *Int. J. Polymer Mater.* **5** (1976) 43.
10. L. D. COXON and J. R. WHITE, *J. Mater. Sci.* **14** (1979) 1114.
11. *Idem, Polymer Eng. Sci.* **20** (1980) 230.
12. G. J. SANDILANDS and J. R. WHITE, *Polymer* **21** (1980) 338.
13. B. HAWORTH, G. J. SANDILANDS and J. R. WHITE, *Plast. Rubber Int.* **5** (1980) 109.
14. J. R. SAFFELL and A. H. WINDLE, *J. Appl. Polymer Sci.* **25** (1980) 1117.
15. H. KOLSKY and A. C. SHEARMAN, *Proc. Phys. Soc.* **55** (1943) 383.
16. S. RAHA and P. B. BOWDEN, *Polymer* **13** (1972) 174.
17. M. M. QAYYUM and J. R. WHITE, unpublished results (1980).
18. J. KUBÁT and M. RIGDAHL, *Int. J. Polymer Mater.* **3** (1975) 287.
19. *Idem, Mater. Sci. Eng.* **21** (1975) 63.
20. J. KUBÁT, M. RIGDAHL and R. SELDÉN, *J. Appl. Polymer. Sci.* **20** (1976) 2799.
21. J. R. WHITE, *Mater Sci. Eng.* **45** (1980) 35.
22. *Idem, J. Mater. Sci.* **16** (1981) 3249.
23. R. G. TREUTING and W. T. READ Jr, *J. Appl. Phys.* **22** (1951) 130.
24. P. SO and L. J. BROUTMAN, *Polymer Eng. Sci.* **16** (1976) 785.
25. B. HAWORTH, MSc thesis, University of Newcastle-upon-Tyne (1979).
26. J. C. M. LI, *Can. J. Phys.* **45** (1967) 493.
27. J. KUBÁT, J. PETERMANN and M. RIGDAHL, *J. Mater. Sci.* **10** (1975) 2071.
28. J. KUBÁT, R. SELDÉN and M. RIGDAHL, *J. Appl. Polymer Sci.* **22** (1978) 1715.
29. N. G. McCRUM, B. E. READ and G. WILLIAMS, "Anelastic and Dielectric Effects in Polymeric Solids", (Wiley, London, 1967).
30. E. PINK, *Rev. Deform. Behav. Mater.* **2** (1977) 37.
31. J. HAUSSEY, J. P. CAVROT, B. ESCAIG and J. M. LEFEBVRE, *J. Polymer. Sci. – Polymer Phys. Ed.* **18** (1980) 311.
32. J. KUBÁT and M. RIGDAHL, *Mater. Sci. Eng.* **24** (1976) 223.
33. *Idem, Phys. Stat. Sol. (a)* **35** (1976) 173.
34. J. KUBÁT and R. SELDÉN, *Mater. Sci. Eng.* **36** (1978) 65.

35. J. KUBÁT, *Makromol. Chem. Suppl.* **3** (1979) 233.
36. E. PINK, V. BOUDA and H. BÄCK, *Mater Sci. Eng.* **38** (1979) 89.
37. J. P. CAVROT, J. HAUSSY, J. M. LEFEBVRE and B. ESCAIG, *ibid.* **36** (1978) 95.
38. E. PINK, *Progr. Colloid and Polymer Sci.* **59** (1975) 81.
39. *Idem, Mater. Sci. Eng.* **22** (1976) 85.
40. E. PINK, H. BÄCH and B. ORTNER, *Phys. Stat. Sol. (a)* **55** (1979) 751.
41. E. PINK and J. D. CAMPBELL, *Mater. Sci. Eng.* **15** (1974) 187.
42. *Idem, J. Mater. Sci.* **9** (1974) 665.

Received 19 November 1980 and accepted 2 March 1981.